Mathematical estimation of stress distribution in normal and dysplastic human hips

B. Mavčič [a], B. Pompe [a], V. Antolič [a], M. Daniel [b], A. Iglič [c,*], V. Kralj-Iglič [a,d]

[a] *Department of Orthopaedic Surgery, Clinical Center, Ljubljana, Slovenia*
[b] *Faculty of Mechanical Engineering, Czech Technical University, Praha, Czech Republic*
[c] *Laboratory of Applied Physics, Faculty of Electrical Engineering, University of Ljubljana, Tržaška 25, SI-1000, Ljubljana, Slovenia*
[d] *Institute of Biophysics, Faculty of Medicine, University of Ljubljana, Ljubljana, Slovenia*

Abstract

By using a mathematical model of the adult human hip in the static one-legged stance position of the body, the forces acting on the hip, peak stress in the hip joint and other relevant radiographic and biomechanical parameters were assessed. The aims were to examine if the peak stress in dysplastic hips is higher than in normal hips and to find out which biomechanical parameters contribute significantly to higher peak stress. The average normalized peak stress in dysplastic hips (7.1 kPa/N) was markedly higher ($\approx$100%) than the average normalized peak stress in normal hips (3.5 kPa/N). The characteristic parameters that contributed to higher peak stress in dysplastic hips included the smaller lateral coverage of the femoral head, the larger interhip distance, the wider pelvis, and the medial position of the greater trochanter. These results are consistent with the hypothesis that stress distribution over weight-bearing surface of the hip joint is the relevant parameter for assessment of the risk for developing coxarthrosis.
© 2002 Orthopaedic Research Society. Published by Elsevier Science Ltd. All rights reserved.

Keywords: Hip dysplasia; Contact stress; Hip joint; Pelvic shape

Introduction

Osteoarthritis can develop as an idiopathic disease; however, subtle abnormalities might be detected in the hip joint prior to the onset of symptoms. Origins of the development of osteoarthritis are ascribed to the metabolic resorption of cartilage and the deformation of anatomical structures [11]. Deviations in the size, shape, mutual proportions or orientation of the acetabulum and femoral head are described as hip dysplasia [9]. Although mostly a pediatric problem, hip dysplasia can persist in untreated or unsuccessfully treated cases as residual hip dysplasia and can eventually lead to cartilage degeneration, presumably due to the pathologically increased stress within the joint. Therefore, hip dysplasia represents an important indication for surgical procedures to reduce hip joint stress, slow down the pathological processes in the hip cartilage and thereby contribute to functional normalization of the joint biomechanics [4,10,32].

In clinical practice, the decision to perform a surgical procedure is based on the clinical status of the patient's hip and on the joint's radiographic appearance (e.g., coxa vara/valga, osteophytes, trabecular trajectories in the femoral head, subchondral sclerosis in the acetabular roof, and the center-edge angle ϑ_{CE}). The center-edge angle [34] is often considered to be the decisive factor, since it correlates with the size of the weight-bearing surface and therefore serves as an indirect measure of hip stress [21,23,25]. Since other geometrical parameters are also of importance in determining the hip stress distribution [7,17,15], a more precise analysis including hip and pelvic geometry could constitute an improvement in the planning procedure for treatment of hip dysplasias.

To the authors' knowledge, a measurement of the stresses in the natural hip joint has been performed in vivo in only a single subject with an implanted partial endoprosthesis containing a stress-measuring device [14]. This kind of measurement is inappropriate in clinical practice, but stresses could be estimated by other means, such as external laboratory measurements combined with a mathematical model [2,18]. Several mathematical approaches have been proposed [3,5,6,16,22,

24,30]. Legal developed a practical method for calculating the contact hip joint stress for a specific case based on equilibrium force analysis in the frontal plane [24]. In this method, the resultant hip joint force was calculated in a static one-legged stance position assuming one effective abductor muscle with an attachment point on the greater trochanter and a certain inclination towards the horizontal plane. Hadley et al. [10] followed a similar approach in which the calculation of the hip contact joint stress distribution was restricted to the simplest case of a uniform contact stress distribution.

Our objective was to use a simple three-dimensional (3D) mathematical model [7,15–18] to evaluate the peak stress in dysplastic hips and then to compare the results with the corresponding results for healthy hips. Within the 3D mathematical model used in this paper the resultant hip joint force $\boldsymbol{R}$ was calculated in static one-legged stance and the calculated contact stress distribution was, in general, non-uniform [7,18]. Geometrical parameters of the hip and pelvis obtained from a standard anteroposterior (AP) radiograph served as input data and were used to rescale the reference 3D coordinates of the muscle attachment points in order to yield the coordinates of the muscle attachment points for an individual person [7]. Due to its resemblance to the mid-stance phase of slow gait, static one-legged stance can be used as a representative body position [13] for patients who usually walk slowly [28]. Radiographic and biomechanical parameters important for the peak stress computation [7,15–18] were also analyzed to determine which geometrical parameters directly contribute to the differences in peak stress between dysplastic and healthy hips.

Patients and methods

We analyzed standard AP radiographs of dysplastic and healthy hips. Patients with dysplastic hips were selected from among the group of patients operated on with a diagnosis of *Dysplasia coxae* at the Department of Orthopaedic Surgery in Ljubljana in the years 1988–1993. The diagnosis of dysplasia was made on the basis of clinical and radiographic evaluation. All patients were operated on due to dysplasia, and the analyzed radiographs were taken prior to the first operation. The small group of hips from male subjects did not allow for gender-matched comparison with healthy hips, therefore only the 47 dysplastic hips from female subjects were included. The sample consisted of 20 right and 27 left hips, and the age of the subjects ranged from 18 to 52 years with a median of 33 years.

The gender- and age-matched control group consisted of subjects who had had a radiograph taken of the pelvic region for reasons other than degenerative hip disease and in whom the pelvic radiograph had shown no signs of hip pathology. This group consisted of 36 hips, 18 right and 18 left, and the age of the subjects ranged from 18 to 41 years with a median age of 33 years.

The contours of the bony structures in each radiograph were put into digital form with a digital graphic board. A computer program (HIJOMO) [7,32,35] was then used to measure the radiographic parameters (Fig. 1): interhip distance (*l*), pelvic height (*H*), pelvic width laterally from the femoral head center (*C*), coordinates of the insertion point of the abductors on the greater trochanter in the frontal plane (point *T*), radius of the femoral head (*r*), and the Wiberg center-edge
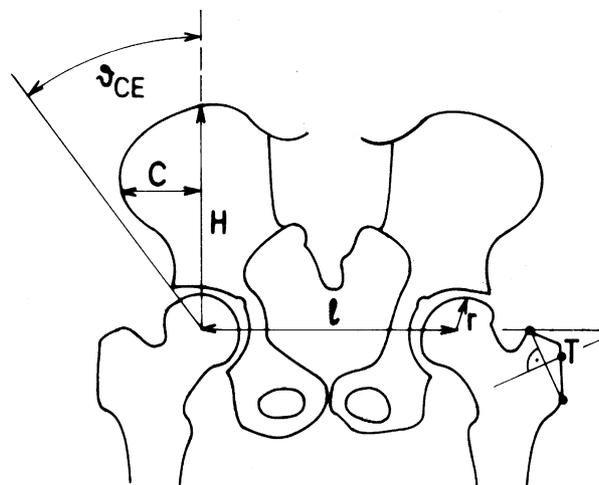

Fig. 1. Pelvic radiographic parameters, *l*, *C*, *H*, and the frontal coordinates of point *T* were used as input data for the computation of the resultant hip force $\boldsymbol{R}$.

angle (ϑ_{CE}) (Fig. 1). The coordinates of point *T* (T_x and T_z) were measured with respect to the femoral head center.

Subsequently a computer program (HIPSTRESS) [15–18,31,34] was used to compute the magnitude and direction of the resultant hip joint force $\boldsymbol{R}$ and the corresponding stress distribution in static one-legged stance. In calculating $\boldsymbol{R}$, the 3D reference coordinates of the muscle attachment points were taken from the work of Dostal and Andrews [8], who performed a case study on one human pelvis and measured 3D coordinates of the abductor muscles. By correcting these 3D coordinates in the medial–lateral and superior–inferior directions with regard to the radiographic pelvic parameters (l, C, H, T_x, T_z), the coordinates of the muscle attachment points for an individual patient were estimated [15–18,31,34]. The model included the unknown forces of the nine hip muscles $\boldsymbol{F}_i$ ($i = 1, 2, \ldots, 9$) with known coordinates for their attachment points ($\boldsymbol{r}_i$) and unknown tensions, the hip load (the weight of the body W_B minus the weight of the loaded leg W_L) originating at the center of the loading mass, and the unknown resultant hip joint force $\boldsymbol{R}$ originating at the femoral head center. The nine model muscles are divided into three muscle groups: anterior, middle and posterior. The average tensions in a particular muscle group were assumed to be equal. In the case of a static one-legged stance, all forces and torques acting in the hip joint are in equilibrium [17]:

$$\sum_i \boldsymbol{F}_i + (W_B - W_L) - \boldsymbol{R} = 0, \tag{1}$$

$$\sum_i \boldsymbol{r}_i \times \boldsymbol{F}_i + \boldsymbol{a} \times (W_B - W_L) = 0, \tag{2}$$

where $\boldsymbol{a}$ is the moment arm of the force ($W_B - W_L$), which is assumed to lie in the frontal plane of the body. The magnitude of the vector $\boldsymbol{a}$ is [28]

$$a = (W_B c - W_L b)/(W_B - W_L), \tag{3}$$

where $b = 0.24l$ and $c = 0.50l$. The solution of the vector equations (1) and (2) yields the three components of the resultant hip force $\boldsymbol{R}$ and the tensions in the abductor muscles [17]. The calculated magnitude and direction of $\boldsymbol{R}$ in all cases turned out to lie nearly in the frontal plane of the body, and its sagittal component did not exceed 1% of the frontal component. The particular choice of the muscles included in the model and the position of the force ($W_B - W_L$) in the frontal plane guaranteed this result.

On the basis of known values of the femoral head radius r, the Wiberg center-edge angle ϑ_{CE}, magnitude of $\boldsymbol{R}$ and inclination of the resultant hip force with respect to the vertical, ϑ_R, the peak stress on the weight-bearing surface, p_{max}, was computed for every individual hip by using another mathematical model [7,16,18]. The model is based on the assumption that the weight-bearing surface in the hip makes part of a perfect articular sphere limited on the lateral side by the

coverage of the acetabulum (ϑ_{CE} angle). Its medial border depends on the location of the pole of stress distribution. With the known magnitude and direction of $\boldsymbol{R}$, the distribution of the contact stress in the hip joint can be computed by integration of the following vector equation over the weight-bearing surface S

$$\int p\, \mathrm{d}\boldsymbol{S} = -\boldsymbol{R}, \tag{4}$$

wherein the value of stress at a given point on the articular surface, p, is proportional to the value of stress at the pole of the stress distribution, p_0 and the cosine of the angle between a given point and the stress pole, γ:

$$p = p_0 \cos \gamma. \tag{5}$$

The solution of the three components of the vector equation (4) with known value of $\boldsymbol{R}$ yields the spherical coordinate of the stress pole (Θ) and the value of stress at the pole p_0 [18]:

$$\vartheta_R + \Theta - \arctan\left(\frac{\cos^2(\vartheta_{CE} - \Theta)}{((\pi/2) + \vartheta_{CE} - \Theta + \frac{1}{2}\sin(2(\vartheta_{CE} - \Theta)))}\right) = 0, \tag{6}$$

$$p_0 = \frac{3R}{2r^2}\left(\frac{\cos(\vartheta_R + \Theta)}{((\pi/2) + \vartheta_{CE} - \Theta + \frac{1}{2}\sin(2(\vartheta_{CE} - \Theta)))}\right) = 0, \tag{7}$$

where it is assumed that the stress pole lies on the lateral side of the contact hemisphere or outside the contact hemisphere in the lateral direction. The solution presented in Eqs. (6) and (7) is the result of the fact that the resultant hip force lies in the frontal plane. If the pole of the stress distribution is located within the weight-bearing surface, the location of p_{max} coincides with the location of the pole (p_{max} equals p_0). When the stress pole lies outside the weight-bearing surface, the stress is maximal at the point on the weight-bearing surface, which is closest to the pole [16,18] (Fig. 2).

The statistical significance of the difference in radiographic and biomechanical parameters between both samples was tested by the unpaired two-tailed Student t-test with unequal variances (limit of significance $p < 0.001$) and the correlation coefficients for the input parameters of the hip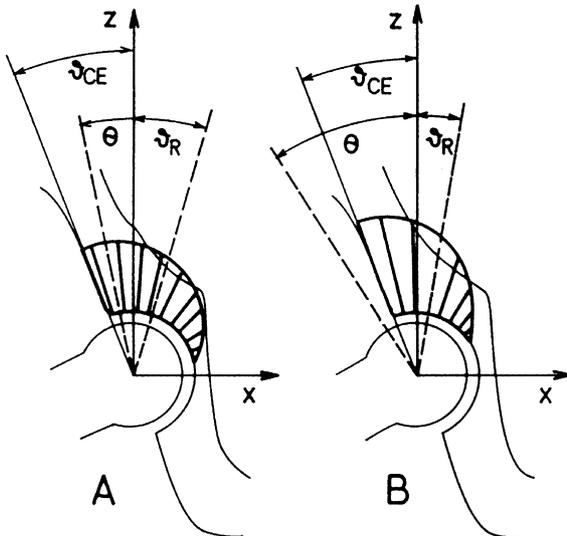 stress model were computed in the following way. As p_{max}/W_B is directly proportional to R/W_B and $1/r^2$ (a linear relationship), the two corresponding correlation coefficients were computed directly. In the case of non-linear dependence between ϑ_{CE} and p_{max}/W_B, we fitted the dependence numerically by using the model equation. The best fit for the dependence between ϑ_{CE} and p_{max}/W_B was computed by using a simple iteration algorithm [20] to find the minimal value of the sum of squares α:

$$\alpha = \sum_{i=1}^{n}(p_{max}(\vartheta_{CEi}, \vartheta_R, r, R/W_B)/W_B - p_{max\,i}/W_B)^2, \tag{8}$$

where i runs over all the data (both the normal and the dysplastic hips). To obtain the minimum value of α, we tried different starting values of variables R/W_B, ϑ_R and r and eventually took into account the optimal solution for the three parameters. The correlation coefficient between the computed values of $p_{max\,i}/W_B$ and the fitted values of $p_{max}(\vartheta_{CEi}, \vartheta_R, r, R/W_B)$ then represented the measure of the influence of the input parameter ϑ_{CE} on the values of p_{max}/W_B. The correlation coefficient for the dependence between ϑ_R and p_{max}/W_B was computed by using the same procedure.

Results

On average dysplastic hips had larger peak stress than healthy hips (Table 1). The values of normalized peak stress in the dysplastic sample were variable and ranged from 2.4 to 22.0 kPa/N. The dysplastic sample mean of 7.1 kPa/N was significantly higher than in the healthy sample, where values ranged from 2.2 to 6.1 kPa/N with a mean of 3.5 kPa/N. The values of peak stress and the resultant hip force were normalized to the body weight of each subject and given as p_{max}/W_B and R/W_B, respectively, as these parameters exhibit the effect of the hip and pelvic geometry [5].

In all parameters except the direction of the resultant hip force ϑ_R and the pelvic width H, the differences between the dysplastic and the healthy group were shown to be statistically significant. However, the parameters where the differences contributed to higher peak stress in the dysplastic group included only ϑ_{CE}, R/W_B, l, T_x and T_z.

The following correlation coefficients for the dependence between the corresponding input parameters and the values of p_{max}/W_B were computed: ϑ_{CE} ($R^2 = 0.81$, $p < 0.001$), ϑ_R ($R^2 = 0.04$, $p = 0.076$), r ($R^2 = 0.09$, $p = 0.007$) and R/W_B ($R^2 = 0.55$, $p < 0.001$). Therefore, ϑ_{CE} exhibited significant correlation with the values of p_{max}/W_B; the correlation of R/W_B (which was in turn computed from l, C, H, T_x, T_z) was less pronounced but still significant. The parameters ϑ_R and r did not correlate significantly with the peak stress.

Discussion

The difference between the dysplastic and healthy hip groups in terms of peak stress p_{max}/W_B was considerable and statistically significant. Mathematical analysis of this biomechanical model has shown [18] that the smaller the arithmetical sum of $(\vartheta_{CE} + \vartheta_R)$, the smaller

Fig. 2. A scheme of the stress distribution in two different hips with equal ϑ_{CE} angle but different ϑ_R angles. The x and z axes of the Cartesian coordinate system lie in the frontal plane of the body while the y axis points in the AP direction. In case A, the ϑ_R is larger, which results in lower peak stress value and more favorable stress distribution with the stress pole located near the acetabular roof. In case B, the angle ϑ_R is smaller, the stress pole is located laterally from the weight-bearing surface, and the peak stress lies at its lateral rim.

Table 1
Radiographic and biomechanical parameters (mean ± std. dev.) in the dysplastic and healthy hip sample groups

Sample group	ϑ_{CE} (°)	l (mm)	C (mm)	H (mm)	T_x (mm)	T_z (mm)	r (mm)	R/W_B ( )	ϑ_R (°)	p_{max}/W_B (kPa/N)
Dysplastic	13 ± 8	208 ± 12	47 ± 10	144 ± 13	14 ± 6	56 ± 6	26 ± 2	3.1 ± 0.3	8 ± 2	7.1 ± 3.7
Healthy	31 ± 6	195 ± 9	56 ± 11	150 ± 10	10 ± 5	61 ± 6	23 ± 1	2.7 ± 0.1	8 ± 1	3.5 ± 0.9
	$p < 0.001$	$p < 0.001$	$p < 0.001$	$p = 0.024$	$p < 0.001$	$p < 0.001$	$p < 0.001$	$p < 0.001$	$p = 0.60$	$p < 0.001$

the radius r, and the larger the magnitude R, the higher the output value of peak stress will be. Our results show that subjects with dysplastic hips have on average smaller angles ϑ_{CE} and larger magnitudes R/W_B, which is consistent with the hypothesis that these two parameters could be responsible for higher stresses in dysplastic hips. In addition, we found strong correlation for the two parameters with the peak stress values. This relationship was not found for the inclination of the resultant hip force ϑ_R, which on average was equal in both populations, while the femoral radius r was even slightly smaller in healthy hips.

In turn, an analysis of the mathematical model for computation of R [7,17] showed that the larger the interhip distance l, the smaller the pelvic height H, the larger the pelvic width laterally from the femoral head center C, the larger the horizontal coordinate T_x and the smaller the vertical coordinate of the insertion point of abductors on the greater trochanter T_z, the larger the magnitude of the resultant hip force R is going to be. Our results confirm that the differences in l, T_x and T_z through a larger magnitude of R contribute to larger stresses in dysplastic hips. However, the values of H did not differ significantly between the two groups, and the values of C were even more favorable in the dysplastic group.

In the past a similar approach was used to estimate the hip joint contact stress from the AP radiographs, where the calculation of the stress distribution was restricted to the case of uniform contact stress distribution [10]. The major advantage of the present method is that it takes into account the non-uniform stress distribution over the weight-bearing surface. This is especially noteworthy, because the gradient of contact stress distribution could be even more important than the magnitude of the contact stress [4]. In our mathematical model, the weight-bearing surface is not fixed in advance. The hip geometry affects the resultant hip force and the size and the shape of the weight-bearing surface in a self-consistent manner [16,18]. The theoretical predictions of the model are based on the assumption of Hooke's law, where the cartilage is described macroscopically as a homogeneous continuum and linear elastic solid. This means that the radial stress in the articular surface was taken to be proportional to the radial strain in the cartilage layer [5]. In fact, the acetabulum is slightly narrower at its edges so as to "hold"

the femoral head in position [29]. In addition, the weight-bearing area is overestimated as a result of ignoring the cotyloid notch. However, this region would not be expected to actually distribute much load [18], therefore the actual overestimation of the contact area is negligible. Also, according to Klaue et al. [19], the planning for hip correction should include assessment of some additional parameters (for example, the posterior femoral cover). The use of standard AP radiographs does not enable computations of these parameters.

Due to the described and other [16,18] simplifications, we could not accurately predict the local contact stress distribution in detail. However, direct measurements in vivo using a specially designed endoprosthesis [14] are consistent with our previous predictions that the peak stress during gait is located in the posterior–medial part of the weight-bearing area of the hip joint [18,26]. In the case of dysplastic hips, the peak stress trajectory is displaced closer to the lateral edge of the acetabulum and anteriorly. Similarly, experimental data based on cadavers [1] show that the location of the peak stress trajectories predicted by our model corresponds to the site where degenerative damage in the hip joint most often occurs.

In direct measurements of peak stress in various activities, e.g. standing up from a chair, peak stress attained up to fivefold higher values relative to the peak stress in static one-legged stance [14]. Using our mathematical model for calculating R does not enable computations of hip forces for such positions of the body and for dynamic activities. In a report of a patient whose hip forces were estimated through laboratory measurements during gait [2], the maximum value of R was in the same range of magnitude as our results. However, the dynamic force R had a considerably large component directed anteriorly. In addition, the inclination of force ϑ_R was significantly higher when compared to our static results. While a number of model refinements are possible, the large differences between normal and dysplastic hips are not likely due to model limitations.

The statistical significance of our results is limited by errors in magnification of the AP radiographs. No radioopaque object of standard length was present in the images to use as a ruler, and the error was probably different for each individual because of differences in magnification. In a recent study [33], we considered normal hips imaged with a piece of metal of known

length positioned by a special screw system to the level of the femoral head centers before making AP radiographs. The magnification varied substantially, but the distribution of the magnifications was normal. Therefore, with regard to the population, the magnification should not affect the relative difference between the average or median values, but would rather increase the error and cause the statistical significance of the difference between the considered populations of dysplastic and normal hips to be smaller. However, in determining peak stress, not all the geometrical parameters are equally important, as the functional relations between them are non-linear. It follows from the mathematical model that stress first depends on the radius of the femoral head, then on the interhip distance, subsequently on the lateral extension of the effective attachment point on the greater trochanter and lastly on the pelvic height and width. For example, if the error made in the determination of the pelvic height is about 15%, only a 2% error in the peak stress would occur [7]. Therefore, within the validity of the model, we expect that the error due to the lack of 3D information in the AP radiograph amounts to about 10%.

Hip joint contact stress is believed to be an important parameter in assessment of hip dysplasia [4,31,34]. The results of our study are consistent with the hypothesis that dysplastic hips have considerably elevated cumulative contact stress overdose [10,27]. The lack of male dysplastic hips in our study did not allow for statistical comparison between female and male hips. Recently the relative maximum hip joint contact stress p_{max}/W_B was found to be higher in healthy women than in healthy men [15]. As women have a higher incidence of arthrosis [12,31], these results support our hypothesis that increased contact stress in the hip joint can be one of the reasons for the development of arthrosis [15]. However, it remains to be seen how the features connected to stress correspond to the other mechanisms occurring in the development of osteoarthritis at the microcellular level [4].

Acknowledgements

References

[1] Afoke NYP, Byers PD, Hutton WC. Contact pressures in the human hip joint. J Bone Joint Surg [Br] 1987;69B:536–41.

[2] Baker KJ, Brown TD, Brand RA. A finite element analysis of intertrochanteric osteotomy on stresses in femoral head osteonecrosis. Clin Orthop 1989;249:183–98.

[3] Brand RA, Pedersen DR, Davy DT, Kotzar GM, Heiple KG, Goldberg VM. Comparison of hip force calculation and measurements in the same patient. J Arthroplasty 1994;9:45–51.

[4] Brand RA, Iglič A, Kralj-Iglič V. Contact stress in the human hip: implications for disease and treatment. Hip Int 2001;11:117–26.

[5] Brinckmann P, Frobin W, Hierholzer E. Stress on the articular surface of the hip joint in healthy adults and person with idiopathic osteoarthrosis of the hip joint. J Biomech 1981;14:149–56.

[6] Dalstra M, Huiskes R. Load transfer across the pelvic bone. J Biomech 1995;28:715–24.

[7] Daniel M, Antolič V, Iglič A, Kralj-Iglič V. Determination of contact hip stress from nomograms based on mathematical model. Med Eng Phys 2001;23:347–57.

[8] Dostal WF, Andrews JG. A three-dimensional biomechanical model of hip musculature. J Biomech 1981;14:803–12.

[9] Durnin CW, Ganz R, Klaue K. The acetabular rim syndrome—a clinical presentation of dysplasia of the hip. J Bone Joint Surg [Br] 1991;73B:423–9.

[10] Hadley NA, Brown TD, Weinstein SL. The effects of contact pressure elevations and aseptic necrosis on the long-term clinical outcome of congenital hip dislocation. J Orthop Res 1990;8:504–13.

[11] Harris WH. Ethiology of osteoarthritis of the hip joint. Clin Orthop 1986;213:20–33.

[12] Heliovaara M, Makela M, Impivaara O, Knekt P, Aromaa A, Sievers K. Association of overweight, trauma and workload with coxarthrosis. A health survey of 7217 persons. Acta Orthop Scand 1993;64:513–8.

[13] Hipp JA, Sugano N, Millis MB, Murphy SB. Planning cetabular redirection osteotomies based on joint contact pressures. Clin Orthop 1999;364:134–43.

[14] Hodge WA, Carlson KL, Fijan RS, Burgess RG, Riley PO, Harris WH, et al. Contact pressures from an instrumented hip endoprosthesis. J Bone Joint Surg [Am] 1989;71A:1378–86.

[15] Iglič A, Daniel M, Kralj-Iglič V, Antolič V, Jaklič A. Peak hip joint contact stress in male and female populations. J Musculoskeletal Res 2001;5:17–21.

[16] Iglič A, Kralj-Iglič V, Antolič V, Srakar F, Stanič U. Effect of the periacetabular osteotomy on the stress on the human hip joint articular surface. IEEE Trans Rehab Eng 1993;1:207–12.

[17] Iglič A, Srakar F, Antolič V. Influence of the pelvic shape on the biomechanical status of the hip. Clin Biomech 1993;8:223–4.

[18] Ipavec M, Brand RA, Pedersen DR, Mavčič B, Kralj-Iglič V, Iglič A. Mathematical modelling of stress in the hip during gait. J Biomech 1999;32:1229–35.

[19] Klaue K, Sherman M, Perren SM, Wallin A, Looser C, Ganz R. Extra-articular augmentation for residual hip dysplasia. J Bone Joint Surg [Br] 1993;75B:750–4.

[20] Kreyszig E. Advanced engineering mathematics. New York: John Wiley & Sons; 1993, p. 650–71.

[21] Kummer B. Biomechanischer Aspekt der Luxationshüfte. Orthopäde 1988;17:452–62.

[22] Kummer B. Die klinische Relevanz biomechanischer Analysen der Hüftregion. Z Orthop 1991;129:285–94.

[23] Larson CB. Rating scale for hip disabilities. Clin Orthop 1963;31:85–93.

[24] Legal H. Introduction to the biomechanics of the hip. In: Tönnis D, editor. Congenital Dysplasia and Dislocation of the Hip. Berlin: Springer-Verlag; 1987. p. 26–57.

[25] Malvitz TA, Weinstein SL. Closed reduction for congenital dysplasia of the hip. J Bone Joint Surg [Am] 1994;76A:1777–91.

[26] Mavčič B, Antolič V, Brand R, Iglič A, Kralj-Iglič V, Pedersen DR. Peak contact stress in human hip during gait. Pflügers Arch—Eur J Physiol 2000;440(Suppl):177–8.

[27] Maxian TA, Brown TD, Weinstein SL. Chronic stress tolerance levels for human articular cartilage: two non-uniform contact

models applied to long term follow up of CDH. J Biomech 1995; 28:159–66.

[28] McLeish RD, Charnley J. Abduction forces in the one-legged stance. J Biomech 1970;3:191–209.

[29] Oberländer W. On biomechanics of joints. The influence of functional cartilage swelling on the congruity of regularly curved joints. J Biomech 1978;11:151–3.

[30] Rappeport DJ, Carter DR, Schurman DJ. Contact finite element stress analysis of the hip joint. J Orthop Res 1985;3:345–446.

[31] Tepper S, Hochberg MC. Factors associated with hip osteoarthritis: data from the First National Health and Nutrition Examination Survey. Am J Epidemiol 1993;137:1081–8.

[32] Vengust R, Daniel M, Antolič V, Zupanc O, Iglič A, Kralj-Iglič V. Biomechanical evaluation of hip joint after innominate osteotomy: a long-term follow-up study. Arch Orthop Trauma Surg 2001;121:511–6.

[33] Vengust R, Drobnič M, Daniel M, Antolič V, Pernuš F, Iglič A, et al. Role of magnification of standard anterior–posterior radiographs in determination of contact hip joint stress. Biomed Eng Appl Basis Commun 2000;12:242–4.

[34] Wiberg G. Studies on dysplastic acetabula and congenital subluxation of the hip joint—with special reference to the complication of osteoarthritis. Acta Orthop Scand 1939;58(Suppl): 1–135.

[35] Zupanc O, Antolič V, Iglič A, Jaklič A, Kralj-Iglič V, Stare J, et al. Assessment of the contact stress in the hip joint after operative treatment of severe slipped capital epiphysis. Int Orthop 2001; 25:9–12.